

Towards CARS-tomography: A comparative Raman and CARS-microscopic study

Anuradha A. Ramoji¹, Christoph Krafft², Tobias Meyer², Nadine Vogler², Denis Akimov², Petra Rösch¹, Michael Schmidt¹, Benjamin Dietzek², Christiane Bielecki³, Andreas Stallmach³, Iver Petersen⁴, Jürgen Popp^{1,2}

¹ Institute of Physical Chemistry, Friedrich-Schiller-Universität Jena, Germany. ² Institute for Photonic Technologies, Jena, Germany.

³ Innere Medizin II, University Hospital, University Jena, Germany. ⁴ Institute of Pathology, University Hospital, University Jena, Germany

Introduction

Tomography is the collective term for 3D-imaging techniques that are generally applied to study morphological and chemical features. These techniques have gained wide recognition as an analytical tool in the field of medicine. Different imaging techniques exist using various contrast mechanism. Some of the imaging techniques are label free whereas others require insertion of labels into the tissue. The label free techniques are based on image contrast, which is tissue specific and provide no further detailed information.

In this study we describe the first steps towards CARS-tomography a technique, which is capable to reveal information on both structural and chemical composition of the tissue. CARS is sensitive to the vibrational signature of the tissues and provides chemical selectivity. In CARS the contrast is based on the Raman scattering of molecules which contain information of vibrations of functional groups in tissue. Hence, CARS offers the possibility to collect the topographical information and distribution of specific biochemical components in less time and in larger area compared with micro-Raman spectroscopy. On the other hand micro-Raman spectroscopy provides full spectral information revealing more details of the tissue composition.

In the present work, for the first time CARS images of colon tissue sections have been measured at different wavenumbers and subsequently compared with micro-Raman images. Analysis has also been carried out by applying univariate and multivariate algorithms to the Raman images.

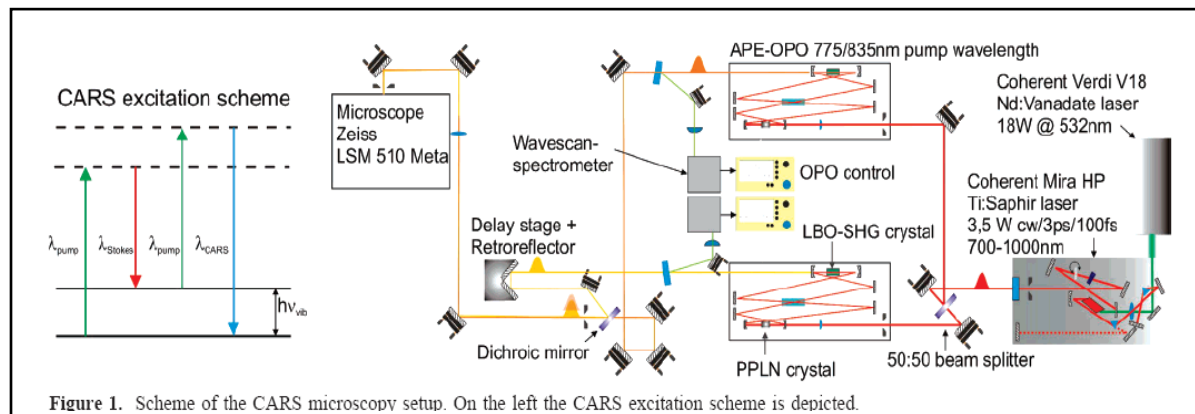
Sample preparation: Tissue specimens were obtained from patients, who were diagnosed with colorectal cancer and subjected to surgery. The colon samples were frozen at -80°C without any fixation. $10\ \mu\text{m}$ tissue sections were prepared using a cryotome, transferred on a quartz slide and dried for Raman spectroscopy. The study protocol was approved by the local ethics commission.

Raman microscopic imaging: Raman spectra were collected at 785 nm laser excitation using Raman system CRM 200 from WITec. A thermoelectrically cooled charge coupled device (CCD) camera was used for detection. The intensity of the laser beam focused on the samples was $\sim 30\ \text{mW}$, a 50x/NA 0.95 objective has been used. Raman images were measured by moving the sample with a motorized stage at a step size of $0.5\ \mu\text{m}$. Spectra were collected in the $200\ \text{to}\ 2000\ \text{cm}^{-1}$ region; for analysis the region $550 - 1800\ \text{cm}^{-1}$ was selected. Acquisition time for each spectrum was 30 s and $\sim 10\ \text{h}$ per scan. The instrument was calibrated using the Raman bands of 4-acetamidophenol.

CARS Microscopy: Fig 1. shows a schematic diagram of the CARS setup. The CARS signal was collected in the forward direction (F-CARS) by an NA 0.55 condenser and detected by photomultipliers (Hamamatsu R6357). Residual pump and Stokes radiation was separated by dielectric filters. CARS images were recorded with a resolution of 512×512 pixels in a total acquisition time of 5.4 s.

Data analysis: Raman images are preprocessed by applying Cytospec program. All spectra were preprocessed using cosmic ray correction followed by baseline correction and vector normalization. Then the data were subjected to k-means cluster analysis in the spectral region $950 - 1750\ \text{cm}^{-1}$.

CARS images were exported as grey scale image files for further processing with the Gnu R software. For different wavenumber ranges several images were taken, from which Raman spectra has been recovered using the following procedure. First, the images are background corrected by dividing by an image-dependent scaling factor to get a similar mean brightness for all the images. Second, the intensity values of each individual image are summed leading to a metric representing the overall brightness and therefore the signal strength of the respective image. The Raman spectrum is finally obtained by plotting the obtained brightness metric for a series of images in the selected wavenumber range against the corresponding Raman shifts. Furthermore, the background corrected images are used to compute difference images, which highlight the difference contrast in a series of images. After brightness correction as described above an image taken at off-resonance conditions is subtracted from all images in one series. The minimum as well as the maximum intensity of the resulting images are computed and the difference images are then globally min-max normalized.



Results and Discussion: The photomicrograph (Fig. 2a) is compared with CARS images (Fig. 2c, 2d). The selected region for the Raman measurements represent the mucosa. Above the mucosa the stromal region is located and below is the non-tissue region. The CARS images have low intensity for the non-tissue region, medium intensity represents the stroma and the high intensity for the mucosa.

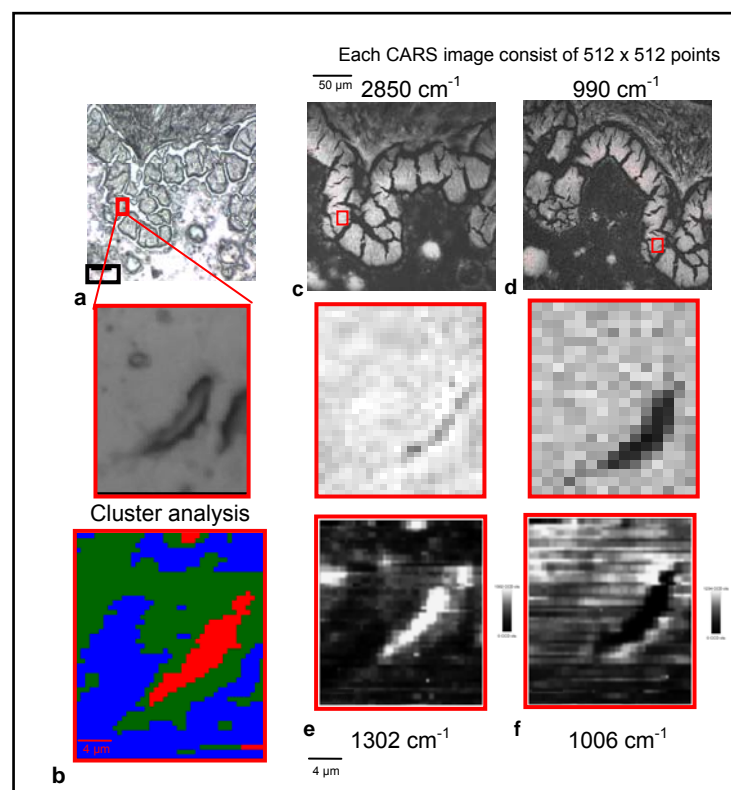


Figure 2. Photomicrograph of colon tissue (a) and k-mean cluster map (b). Analysis of 42×48 Raman map was restricted to the spectral region $950\text{-}1750 \text{ cm}^{-1}$. Comparison of CARS image (c,d) with Raman images displaying the integrated intensity for the respective bands (e,f). (For the sake of comparison, the images in the second row show the magnified area selected for Raman measurement)

The contrast generated in the CARS image is a result of resonant and non-resonant contributions giving molecular and morphological information, respectively. Hence in the stromal region the spectral contributions of proteins dominate whereas the mucosa has a more complex composition including a higher lipid content.

The Raman image (Fig. 2b) of the tissue area indicated by the red box in the photomicrograph (Fig. 2a) consists of 42×48 spectra. The chemical image (Fig. 2e) of the integrated intensity at 1302 cm^{-1} resolves the crack which is intense compared to the surrounding and appears to be filled with lipid. The magnified portion of the CARS image (Fig. 2c) also shows a similar feature when the Stokes laser is tuned to 2850 cm^{-1} . Since the bands at 1302 and 2850 cm^{-1} probe the same chemical entity; CH_2 vibrations of lipids, the former corresponds to the deformation and the latter belongs to the stretching vibrations. Similarly, in (Fig. 2f) the crack is hollow and appears to be empty and the same effect is seen in the magnified CARS image (Fig. 2d) when the Stokes laser is tuned to 990 cm^{-1} .

The composition of the central feature was not clear by the univariate method. Therefore, a multivariate algorithm; k-means clustering in the wavenumber interval 950 to 1750 cm^{-1} was applied. The Raman image is segmented into three clusters (Fig. 2b). Most spectra were assigned to green and blue clusters and the central cut is assigned to the red cluster. The unnormalized mean cluster spectra of Fig. 2b are plotted in Fig. 3A. Spectral contributions of quartz were compensated by subtracting a Raman spectrum of the substrate material.

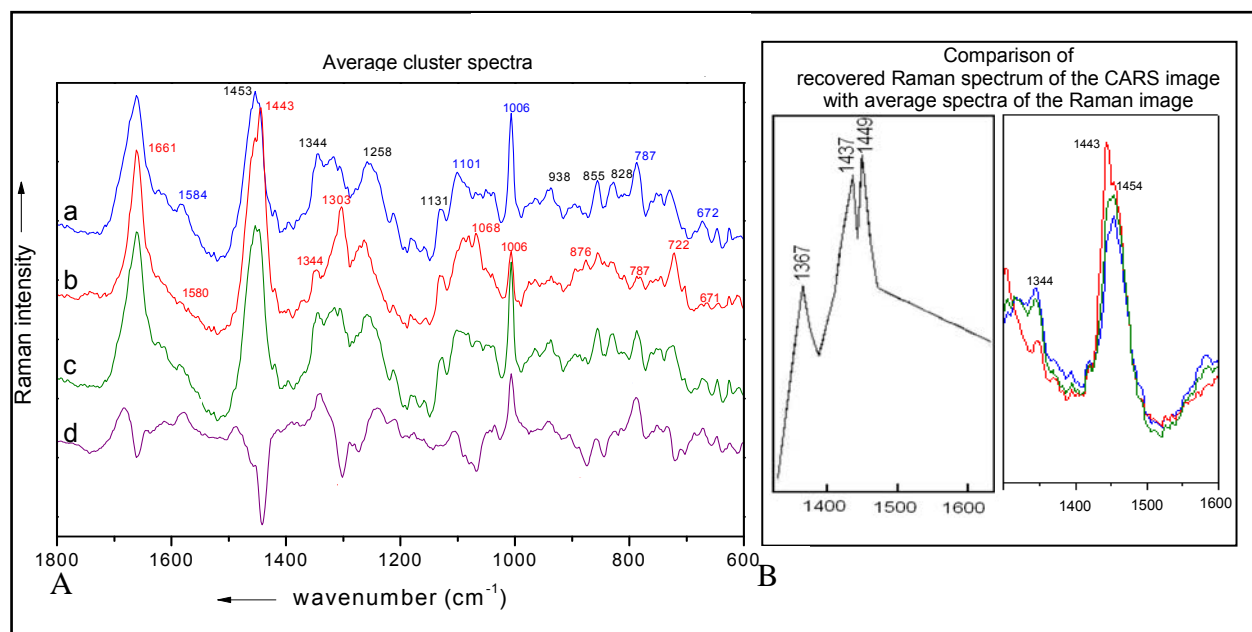


Figure 3. A) displays average k-mean cluster spectra; spectrum-a belongs to blue cluster, b-red cluster, c-green cluster of the image in Fig 2b, spectrum d is difference spectrum of blue and red cluster (a-b). B) gives comparison of the recovered Raman spectrum from CARS and the average spectra of the Raman image in the spectral region 1332-1629 cm^{-1} .

Raman bands in the spectrum of the blue and green clusters are assigned to the peptide group in proteins (938, 1258, 1661 cm^{-1}), aromatic amino acid side chains (828, 855, 1006, 1344 cm^{-1}), aliphatic amino acid side chains (1131, 1344, 1453 cm^{-1}) and nucleic acids (672, 787, 1101, 1584 cm^{-1}). Numerous changes are observed in the Raman spectrum of the red cluster, most significantly lower intensities at 671, 787, 1006, 1344 and 1580 cm^{-1} and higher intensities at 722, 876, 1068, 1303, 1443 and 1661 cm^{-1} . The increased bands point to high content of unsaturated lipids, in particular phosphatidylcholine, the decreased bands to lower protein and nucleic acid contents. A difference spectrum was calculated between the spectrum of the blue cluster (a) and the spectrum of the red cluster in Fig. 2A. After normalization to the band 1006 cm^{-1} , the negative difference band near 720, 874, 1068, 1301, 1442, 1661 cm^{-1} indicates to the high lipid content in the spectrum of red cluster and the positive bands at 672, 788, 1006, 1341 and 1578 cm^{-1} indicates the nuclei acids and proteins contribution in the spectrum of blue cluster. The spectral information of a series of CARS images from 1332 to 1629 cm^{-1} has been reconstructed as plotted in Fig 3B.

Conclusion: CARS images were measured for different Stokes lines; selective protein and lipid bands were resonantly probed. The CARS images correlate well with the Raman images. The acquisition time required to measure a Raman image was longer than the CARS image but Raman spectroscopy gives full spectral information. Raman images were analyzed using multivariate statistical methods. The chemical selectivity in CARS microscopy combined with Raman technique has promising future in tissue pathology and in clinical applications. Details of this study will be published (Krafft, Ramoji et al., J. Biophoton. (accepted)).

Acknowledgement: Funding of the research project Exprimage (FKZ 13N9364) within the framework 'Biophotonik' from the Federal Ministry of Education and Research, Germany (BMBF), the EFRE project, the Photonics4life network (Grand Agreement no.: 224014) are gratefully acknowledged.